Structural, spectroscopic, and electrochemical behavior of *trans*-phenolato cobalt(III) complexes of asymmetric NN′O ligands as archetypes for metallomesogens

Rajendra Shakya,[a] Camille Imbert,[a] Hrant P. Hratchian,[a] Mauricio Lanznaster,[a] Mary Jane Heeg,[a] Bruce R. McGarvey,[b] Marco Allard,[a] H. Bernhard Schlegel[a] and Claudio N. Verani*[a]

Received 6th October 2005, Accepted 10th February 2006
First published as an Advance Article on the web 3rd March 2006
DOI: 10.1039/b514190g

In order to understand and predict structural, redox, magnetic, and optical properties of more complex and potentially mesogenic electroactive compounds such as $[Co^{III}(L^{t\text{-}BuLC})_2]ClO_4$ (**1**), five archetypical complexes of general formula $[Co^{III}(L^{RA})_2]ClO_4$, where R = H (**2**), *tert*-butyl (**3**), methoxy (**4**), nitro (**5**), and chloro (**6**), were obtained and studied by means of several spectrometric, spectroscopic, and electrochemical methods. The complexes **2**, **4**, and **6** were characterized by single-crystal X-ray diffraction, and show the metal center in an approximate D_{2h} symmetry. Experimental results support the fact that the electron donating or withdrawing nature of the phenolate-appended substituents changes dramatically the redox and spectroscopic properties of these compounds. The $3d^6$ electronic configuration of the metal ion dominates the overall geometry adopted by these compounds with the phenolate rings occupying *trans* positions to one another. Formation of phenoxyl radicals has been observed for **1**, **3**, and **6**, but irreversible ligand oxidation takes place upon bulk electrolysis. These data were compared to detailed B3LYP/6-31G (d)-level computational calculations and have been used to account for the results observed. A comparison between compound **1** and archetype **3**, validates the approach of using archetypical models to study metal-containing soft materials.

Introduction

Interest in metal-containing soft materials has increased due to applications towards molecular electronics[1] and magnetic films.[2] These materials are usually composed of an organic fragment attached to a ligand capable of coordinating metals. Rigid ligands such as terpy (2,6-di(pyridin-2-yl)pyridine) and R_2bzimpy (2,6-bis[*N*′-R-benzimidazol-2-yl]pyridine, R = H, Me) have been used to append different groups, thus forming building blocks for molecular transistors,[3] polymers,[4] liquid crystals,[5] and plastics.[6] More flexible alkylpyridyl ligands have been used for sensing purposes,[7–9] whereas asymmetric tridentate ligands remain largely unexplored. The design of soft materials based on these ligands leads to unique physical properties associated with dissimilar donor sets and metallation is expected to allow for some control over the final behavior of these materials.[10] Our group is interested in soft materials with electroactive and metallomesogenic properties as alternatives to phase-dependent spin-crossover switching.[1] The ground state switching mechanism in such metallomesogens is supposedly phase-independent, thus broadening the potential for molecular electronic applications. Ongoing research in our laboratories focuses on asymmetric ligands with pyridine and phenol pendant-arms, and we have developed a new ligand $HL^{t\text{-}BuLC}$ along with its first cobalt complex $[Co^{III}(L^{t\text{-}BuLC})_2]ClO_4$ (**1**). Compound **1** was thoroughly characterized and exhibited a complex electrochemical behavior, but attempts to obtain crystallographic information failed. In order to model and predict the behavior of this class of metal-containing soft material, we have followed the widely accepted bioinorganic approach of using model complexes to mimic structural and electronic properties of active centers in enzymes.[11] In this bioinspired approach, we investigated a series of discrete archetypical complexes $[Co^{III}(L^{RA})_2]ClO_4$ that retain key attributes of **1** (Scheme 1), by means of mass spectrometry, vibrational, electronic, and EPR spectroscopy, and electrochemical methods. The results obtained from these archetypes will allow us to infer important characteristics of **1** leading to a better understanding of its behavior, as well as a more rational approach to the synthesis and expected properties of similar materials. Complexes **2**, **4**, and **6**

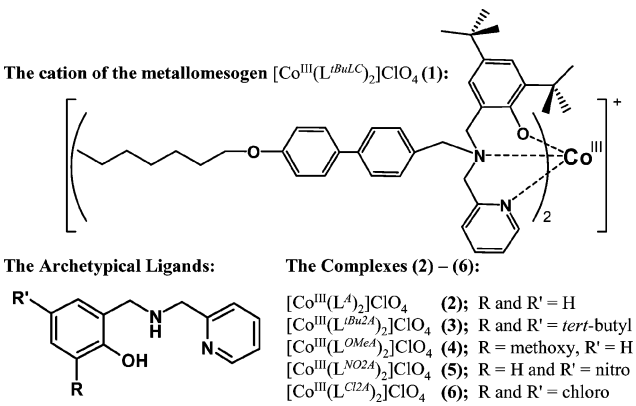

Scheme 1

[a]*Department of Chemistry, Wayne State University, 5101 Cass Ave., Detroit, MI 48202, USA. E-mail: cnverani@chem.wayne.edu*
[b]*Department of Chemistry and Biochemistry, University of Windsor-401 Sunset Ave., Windsor, ON N9B 1P4, Canada*

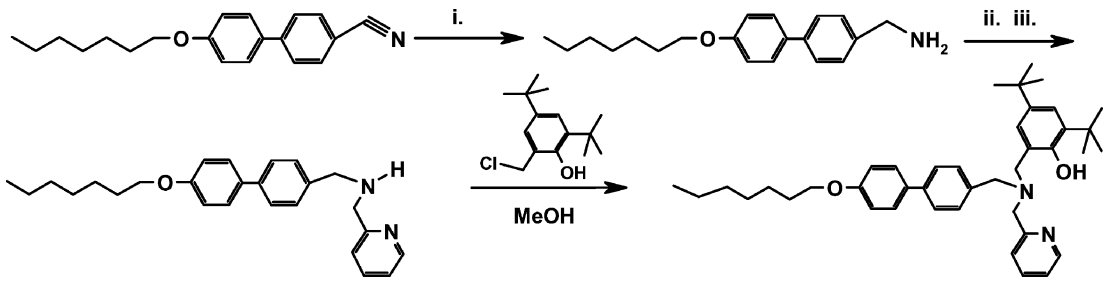

Fig. 1 Synthesis of the ligand $HL^{t\text{-}BuLC}$. (i) Nitrile reduction by $LiAlH_4$ in THF; (ii) Schiff-base condensation with 2-pydinecarboxyaldehyde in MeOH followed by (iii) reduction with $NaBH_4$.

were studied by X-ray crystallography, and experimental trends are analyzed *via* computational calculations. Comparisons between compound **1** and the archetype **3** are included.

Results and discussion

Syntheses and characterizations

The ligand $HL^{t\text{-}BuLC}$ was synthesized by treatment of *para*-(heptyloxy)benzenaniline with 2-pyridinecarboxyaldehyde followed by reduction and treatment with 2,4-di-*tert*-butyl-6-(chloromethyl)phenol as indicated in Fig. 1. The archetypical ligands were obtained by Schiff-base condensation of appropriately substituted salicylaldehydes and aminomethyl-pyridine in MeOH followed by reduction with $NaBH_4$ yielding HL^{A}, HL^{tBu2A} and HL^{Cl2A} with *ortho*- and *para tert*-butyl and chloro groups respectively, HL^{OMeA} with an *ortho*-methoxy group, and HL^{NO2A} with a *para*-nitro group. The ligands were characterized by ^{1}H-NMR, ESI mass spectrometry, and IR spectroscopy, with overall yields of 80–85%.

Compound **1** was obtained as a waxy material upon treatment of the ligand $HL^{t\text{-}Bu2LC}$ with hexahydrated cobalt(II) perchlorate in MeOH using triethylamine as base and was characterized by IR and UV-visible spectroscopy, and mass analysis. Attempts to obtain the elemental analysis of **1** failed. Nonetheless, the presence of vibrational modes associated with the ligand, mainly those related to C–H stretching of the tertiary butyl and heptyl groups along with perchlorate counterions, clearly indicates complex formation. Additionally, the ESI mass analysis of **1** shows a prominent peak cluster at $m/z = 1270$ indicating the formation of the cationic species $[Co^{III}(L^{t\text{-}BuLC})_2]^+$. No evidence of multimetallic species was found and the nature of the metal ion is confirmed by the simulation of the isotopic distribution of the above mentioned cluster (Fig. 2).

The peak pattern for **1** is in excellent agreement with the pattern observed for archetype **3** and consistent with other compounds discussed here. These data support a complex formed with a 2 : 1 ligand : metal ratio. The study of the potential metallomesogenic properties of $\mathbf{1}^+$ is under development with different counterions to avoid the risks involved with perchlorate chemistry. The results shall appear in a separate account. Complexes **2–6** were synthesized in a similar way and all complexes show good elemental analyses and well defined $m/z = [M^{III}(L)_2]^+$ peaks in MeOH, as observed by ESI mass spectrometry in the positive mode. Peak simulation showed good agreement between position and isotopic distributions.[12] The analyses suggest that these complexes retain their structure both in solution and as a solid, as expected for hexacoordinate complexes of an inert $3d^6$ ion. All complexes present a perchlorate counterion found at 1116–1088 cm^{-1} in the IR spectrum.

Molecular structures

The molecular structures of archetypes **2**, **4**, and **6** were determined by X-ray diffraction of monocrystals grown from MeOH. Fig. 3 displays the ORTEP diagrams of the complex cations and Table 1 shows selected bond lengths and angles. All three structures are composed of pseudo-octahedral cations with the Co(III) ion surrounded by two facially-coordinated and deprotonated ligands $(L^{RA})^-$ with R = H, MeO, and Cl for **2**, **4**, and **6** respectively. Complex **2** presents a single discrete cationic species in its unit cell, whereas **4** exhibits two cations (indicated as #1 and #2) and three cations are observed for **6** (indicated as #1, #2, and #3). In each of these cations the tridentate ligands adopt a *sym-fac* coordination,[13] and the cobalt ions are in an exact or pseudo centrosymmetric environment described in a Bailar, Miessler, and Tarr notation[14] as $[Co\langle N_{am1}N_{am2}\rangle\langle N_{py1}N_{py2}\rangle\langle O_{phen1}O_{phen2}\rangle]$. The equivalent donor sets in both ligands are *trans* to each other and the distances and angles are in good agreement with the values expected for coordination of the N_{am}, N_{py}, and O_{phen} donor sets with a low-spin cobalt(III) ion with *trans*-phenolate geometry.[15] The $Co–O_{phenolate}$ distances range from 1.988 to 1.920 Å, with **6**

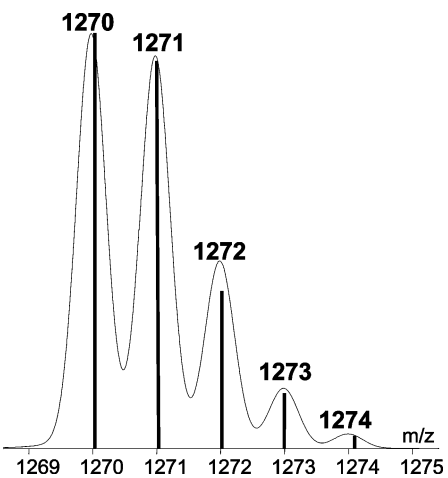

Fig. 2 Isotopic distribution for **1**. Bar cluster: experimental. Continuous spectrum: simulated cluster.

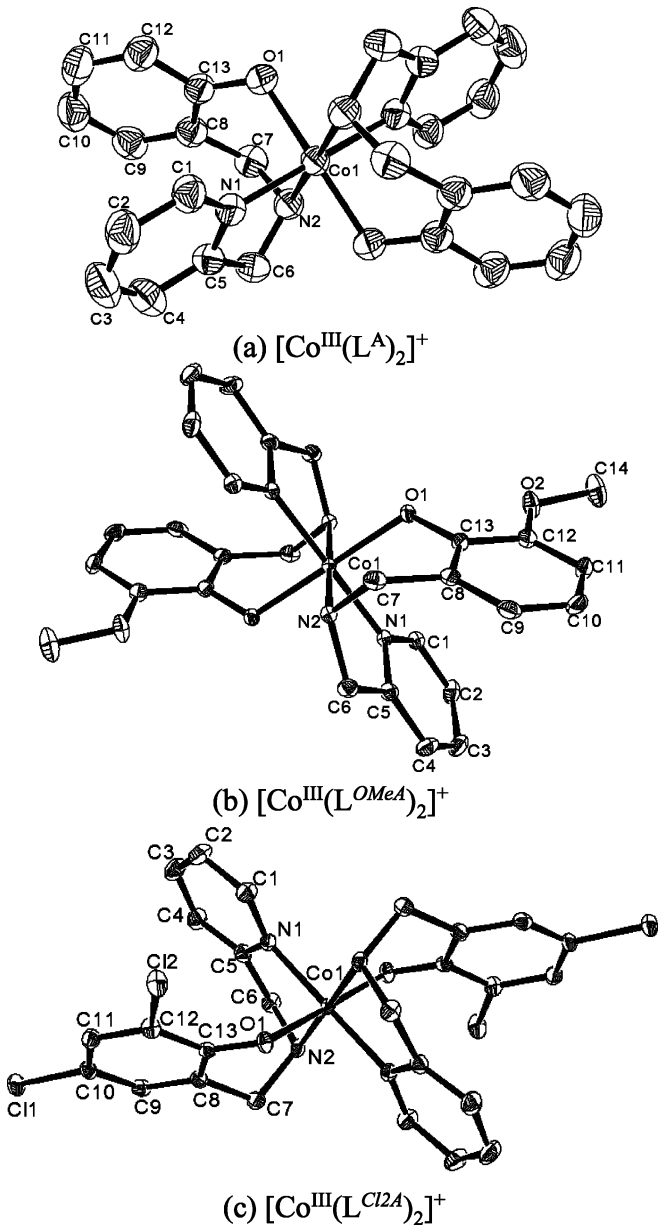

Fig. 3 ORTEP representations at 50% probability for the cations of complexes (a) **2**, (b) **4**, and (c) **6**. Counterions, solvents, and hydrogen atoms excluded for clarity.

grouping at the low end of this range, thus consistent with the presence of two electron-withdrawing chloro substituents on each phenolate ring. The Co–N_{amine} and Co–$N_{pyridine}$ distances show less variation and range from 1.946 to 1.964 Å. Ordered perchlorate anions are also present and show Cl–O bonds ranging from 1.412 to 1.428 Å. In contrast to the described *sym-fac* coordination for these ligands with the cobalt(III) ion, we have recently reported on the *unsym-fac* coordination mode for iron(III) complexes[16] with the ligands $(L^{A})^{-}$ and $(L^{t\text{-}Bu2A})^{-}$. The iron(III) complexes are described as $[Fe\langle N_{am1}O_{phen2}\rangle\langle N_{am2}O_{phen1}\rangle\langle N_{py1}N_{py2},\rangle]$, thus displaying a *cis*-arrangement of the phenolate rings, with the Fe(III) center in an approximate C_{2v} symmetry. For structures **2**, **4**, and **6** the cobalt(III) center adopts an approximate D_{2h} symmetry in which the orbitals $d_{x^2-y^2}$ and d_{z^2} transform as a_g, whereas d_{xy}, d_{xz} and d_{yz} transform respectively as b_{1g}, b_{2g}, and b_{3g}. In order to further understand the *cis*/*trans* geometric preferences observed in these complexes, computational calculations were performed and analyzed (*vide infra*).

UV-visible spectroscopy

The spectra of the archetypical ligands and of compound **1** were taken in CH_2Cl_2, and the spectra of archetypes **2–6** were taken in 1 : 1 mixtures of CH_2Cl_2–CH_3OH to assure homogeneity of all solutions. The apparent lower extinction coefficients observed for **1** when compared to **2–6** are due to the higher molecular mass of the former species. Table 2 summarizes the results and Fig. 4 shows spectra of the complexes. Intense $\pi \rightarrow \pi^*$ intraligand bands were observed in the UV region for **1–6**, whereas $p\pi_{phenolate} \rightarrow d\sigma^*_{cobalt(III)}$ charge transfer bands were found between 430 and 470 nm for all complexes, thus in good agreement with values reported in the literature.[14] Comparison between unsubstituted and *tert*-butyl-substituted species shows this LMCT band shifting from 431 nm in **2** to 470 nm in **3**. Therefore, the latter archetypical complex models the behavior of compound **1**, were this transition is observed at 466 nm. Similar trends were observed for previously reported iron compounds with comparable ligands.[15] Complex **5** presents a broad $p\pi_{phenolate} \rightarrow p_{NO2}$ intraligand charge transfer band at 377 nm that superimposes the $p\pi_{phenolate} \rightarrow d\sigma^*_{cobalt(III)}$ transition, preventing further discussion. This band has been observed for the protonated and non-metallated ligand at 323 nm. The presence of several independent cations observed in the crystal structures of **4** and **6** do not pose a problem to the UV-visible studies because the cations are expected to assume similar and averaged bond lengths and angles when in solution. The low spin character of these species was confirmed by EPR spectroscopy and the six electrons of a cobalt(III) center in a D_{2h} symmetry will be described by a $[b_{1g}^2, b_{2g}^2, b_{3g}^2, a_g^0, a_g^0]$ configuration. Dominant σ-bonding interactions will arise because d–d transitions are low in intensity and occupation of the b_{1g}, b_{2g}, and b_{3g} orbitals precludes the presence of strong π-bonds, as supported by the relatively long Co–O bonds observed for **2**, **4**, and **6**. Compound **1** and archetypes **2–6** also exhibit a transition between 560 and 670 nm. This band

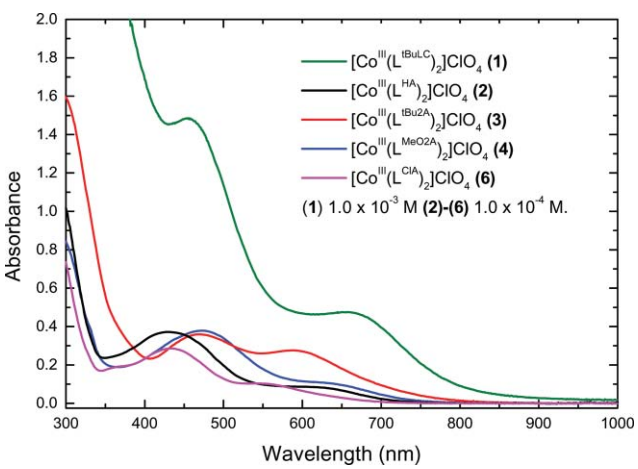

Fig. 4 UV-visible spectra of complexes **1–6** in CH_2Cl_2.

Table 1 Selected bond distances (Å) and angles (°) for **2**, **4**(#1), and **6**(#1)

$[Co^{III}(L^{A})_2]ClO_4$ (**2**)		$[Co^{III}(L^{OMeA})_2]ClO_4 \cdot H_2O$ (**4**) Cation #1		$[Co^{III}(L^{Cl2A})_2]ClO_4$ (**6**) Cation #1	
Co1–O1	1.9158(12)	Co1–O1	1.9204(15)	Co1–O1	1.8986(13)
Co1–N2	1.9624(15)	Co1–N2	1.9590(18)	Co1–N2	1.9573(16)
Co1–N1	1.9563(15)	Co1–N1	1.9484(18)	Co1–N1	1.9611(16)
O1–C13	1.338(2)	C13–O1	1.347(2)	C13–O1	1.321(2)
C7–C8	1.493(3)	C7–C8	1.500(3)	C7–C8	1.506(3)
C7–N2	1.495(3)	C7–N2	1.492(3)	C7–N2	1.497(3)
N2–C6	1.477(3)	N2–C6	1.485(3)	N2–C6	1.490(3)
C5–C6	1.491(3)	C5–C6	1.493(3)	C5–C6	1.495(3)
Bite angles:					
O1–Co1–N2	94.28(6)	O1–Co1–N2	94.48(7)	O1–Co1–N2	94.68(6)
N2–Co1–N1	82.84(7)	N1–Co1–N2	84.70(8)	N1–Co1–N2	84.65(7)
Average distances:					
C–C in Py	1.375(9)	C–C in Py	1.383(3)	C–C in Py	1.383(4)
C–N in Py	1.343(3)	C–N in Py	1.350(4)	C–N in Py	1.350(4)
C–C in Ph	1.389(12)	C–C in Ph	1.395(13)	C–C in Ph	1.393(13)
				C–Cl	1.742(4)

Table 2 UV-visible and electrochemical parameters for ligands and complexes

	λ/nm (ε/L mol^{-1} cm^{-1})[a]	$E_{1/2}{}^1$/V (ΔE/V)[b]	$E_{1/2}{}^2$/V (ΔE/V)	$E_{1/2}{}^3$/V (ΔE/V)
HL^{A}	262 (4500); 268 (4350); 278 (3150); 332 (190)	Irreversible behavior		
$HL^{t\text{-}BuA}$	262 (3750); 268 (3550); 282 (2990)	—	0.33 (0.19)	0.84 (0.39)
HL^{OMeA}	262 (3930); 281 (2650)	Not measured		
HL^{NO2A}	262(5040); 323 (11 100)	Not measured		
HL^{Cl2A}	262 (3680); 293 (2980)	Not measured		
$[Co(L^{t\text{-}BuLC})_2]ClO_4$ (**1**)	466 (1463); 672 (495)	−0.83(0.26)	0.38 (0.14)	
$[Co(L^{A})_2]ClO_4$ (**2**)	261sh (11 240); 282 (10 680); 431 (2770); 623 (910)	−0.91(0.30)	—	—
$[Co(L^{t\text{-}BuA})_2]ClO_4$ (**3**)	251sh (19 110); 289 (16 250); 470 (3590); 589 (2080)	−0.90(0.38)	0.43 (0.10)	0.78 (0.10)
$[Co(L^{MeOA})_2]ClO_4$ (**4**)	292 (9140); 471 (3790); 637 (1023)	−0.88(0.13)	—	—
$[Co(L^{NO2A})_2]ClO_4$ (**5**)	228 (18 650); 369 (15 780): 607 (402)	−0.55(0.13)	—	—
$[Co(L^{Cl2A})_2]ClO_4$ (**6**)	258 (12 450); 286sh (9618); 431 (2850); 564 (966)	−0.67(0.20)	0.87 (0.09)	1.29 (0.14)

[a] Spectra measured in CH_2Cl_2 for ligands and **1**. Spectra in CH_2Cl_2–MeOH (1 : 1) for **2–6**. [b] All CVs measured in CH_2Cl_2, with $TBAPF_6$ as the supporting electrolyte. Scan rate of 100 mV s^{-1} at RT using a three electrode system (glassy carbon, Ag/AgCl, Pt wire). Potentials referenced *vs* the ferrocenium/ferrocene couple.

has been attributed to the d–d transition $^1A_{1g} \rightarrow {}^1T_{2g}$,[14] but some caution is necessary since none of the compounds studied here or in the cited reference belong to a genuine O_h point group. Even considering that the $^1T_{2g}$ term splits into $^1A_1 + {}^1B_1 + {}^1B_2$,[17] this band is too intense for a pure d–d transition.

Electrochemistry and EPR spectroscopy

Compound **1** and archetypes **2–6** had their electrochemistry measured in CH_2Cl_2, and the data are shown in Table 2. Compound **1** is characterized by a complex electrochemical behavior that involves a quasi-reversible reduction at −0.83 V *vs* Fc^+/Fc attributed to the Co(III)/Co(II) pair and several irreversible follow-up oxidations attributed to the ligand. If the oxidation stops immediately after the first oxidative process, reversibility is attained. Since this process presents *ca* twice the peak current of the metal-centered process, it might be associated to a 2e$^-$-process,[18] but further investigation is needed in order to firmly establish the number of electrons transferred. The Co(III)/Co(II) reduction is observed between −0.55 and −0.90 V *vs* Fc^+/Fc for archetypes **2** to **6**, spanning a 0.36 V window. It follows the expected trend that electron-donating substituents will increase electronic density around the metal center decreasing the redox potentials, whereas electron withdrawing groups will increase these potentials.[19] It has been suggested[20] that such a large window indicates occupation of a $d_{x^2-y^2}$ orbital of the metal upon reduction. It reflects the occupation of an a_g molecular orbital with $d_{x^2-y^2}$ character in these D_{2h} species. Calculations support this trend and will be detailed later in this paper. Interestingly, only **3** and **6** with respectively appended *tert*-butyl and chloro groups show reversible or quasi-reversible ligand-centered processes as seen in Fig. 5. Compound **3** shows processes at 0.43 and 0.78 V, while **6** exhibits much more

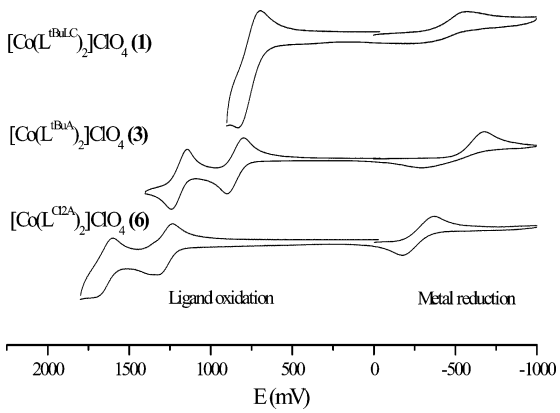

Fig. 5 Cyclic voltammograms of **1**, **3**, and **6** in CH_2Cl_2.

positive values. Such processes fall within the range expected for the conversion of coordinated phenolates into phenoxyl species.[21] The archetype **3** was able to model the behavior of compound **1** in regard to potentials and quasi-reversibility of the metal-centered reductive process. The behavior of the oxidative processes is more complex, because **3** presents two independent waves while **1** displays a multielectron process. Nonetheless, the archetypical compound **3** gave pertinent information about the oxidative potentials. At this point, it is not clear why the appended liquid crystalline group in **1** causes such changes.

Electrolyses at controlled potentials in CH_2Cl_2 solutions were carried out for **3** and **6** to confirm the nature of these processes. Aliquots were isolated under anaerobic conditions before and after the electrolysis and EPR spectra were measured at 120 K. Complexes **3** and **6** present silent spectra before the electrolysis, thus supporting the expected low-spin configuration for the $3d^6$ ions. Upon electrolysis of the first and second oxidative processes (at 1.05 V and 1.40 V respectively) an initial EPR signal is observed at 3300 G with $g = 2.004$ for **3**, as expected for a phenoxyl radical. However, a broader signal with a 35 G line-width is also present overtaking the previous signal toward the end of the electrolyses (Fig. 6). This signal is suggested to arise from a free radical on a nitrogen atom; such radicals have a nitrogen hyperfine interaction of *ca* 15 G which gives a three line pattern about 30 G. A similar behavior was observed for **6**. Post-electrolysis voltammetry reinforces the decomposition of **3** and no further analyses were taken.

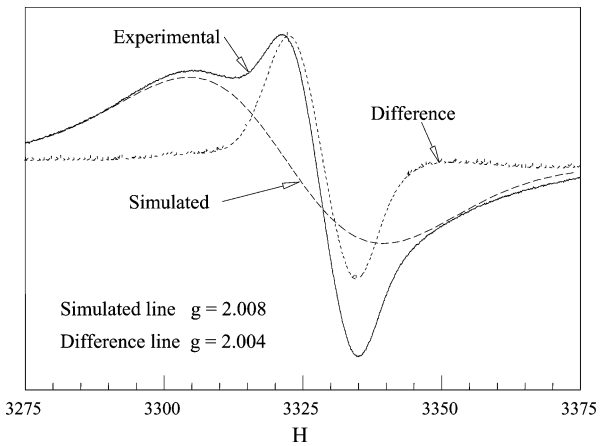

Fig. 6 EPR of the product from the oxidative electrolysis of **3** at 1.40 V.

Electronic structure calculations and analysis

We have recently reported on iron(III) and gallium(III)[16] complexes with similar imine and amine ligands and we have shown that tertiary-butyl groups play a pivotal role in the stabilization of phenoxyl radicals. In the same account we have shown that the phenolate rings adopt a *cis*-configuration in Fe(III) and Ga(III) complexes. Here, we were interested in assessing the energetics related to the preferential *trans* coordination of the phenolate arms in the Co(III) compounds described in this work, as well as in performing an electronic structure analysis to obtain a clear description of the molecular orbitals in compounds **2**–**6**. Calculations were carried out using the GAUSSIAN suite of electronic structure programs.[22] The B3LYP/6-31G(d) level of theory[23] was employed throughout these and the previously published calculations. Standard methods[24] were used to fully minimize structures without symmetry constraints and located stationary points were characterized by analytic vibrational frequencies. Reported energies include the zero-point vibrational correction. Preliminary calculations on the full structures of **2**–**6** yielded similar results to $[Co^{III}(L^A)_2]^+$. Therefore, we consider $[Co^{III}(L^A)_2]^+$ a suitable model for this set of complexes and restrict our discusion in this section to this model structure as a representative case for **2**–**6**. The cation $[Co^{III}(L^A)_2]^+$ can adopt two configurations; one given by $[\langle N_{am1}N_{am2}\rangle\langle N_{py1}N_{py2}\rangle\langle O_{phen1}O_{phen2}\rangle]$ referred to as "*trans-phenolates*," and another given by $[\langle N_{am1}O_{phen2}\rangle\langle O_{phen1}N_{am2}\rangle\langle N_{py1}N_{py2}\rangle]$ called "*cis-phenolates.*" The structures of **2**, **4**, and **6** present a "*trans-phenolates*" configuration. Relative energies for *cis*- and *trans*-phenolates $[Co(L^A)_2]^+$ are shown together with minimized structures in Fig. 7. Calculated energies show that the *trans*-configuration is favored by *ca* 4 kcal mol^{-1}, and in spite of a relatively small energy difference, the results are in good agreement with the trends observed experimentally.

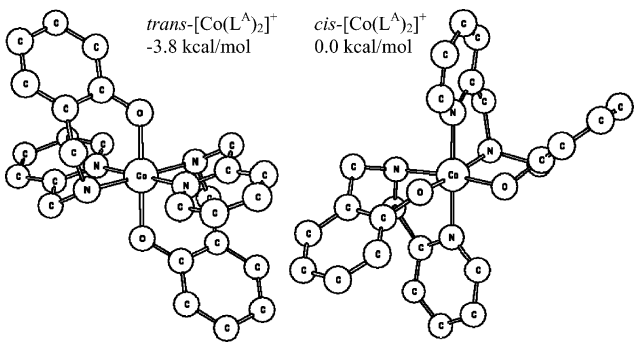

Fig. 7 B3LYP/6-31G(d) minimized geometries and energies for *trans*- and *cis*-$[Co(L^A)_2]^+$. H atoms have been omitted for clarity.

A qualitative molecular orbital description of these compounds has been drawn using the partitioning scheme of Whangbo, Schlegel, and Wolfe,[25] and includes Mulliken molecular orbital percent compositions in terms of fragment orbitals. Two fragments have been defined: (i) the cobalt(III) center and (ii) the ligands. Results for the *trans*- and *cis*-configurations are summarized in Table 3. The *trans*-configuration of $[Co(L^A)_2]^+$ belongs to the pseudo point group D_{2h}, and symmetry assignments are based on the transformations of ligand and metal orbital symmetry adapted linear combinations (SALCs) in this group. The *cis*-configuration suggests a D_{2v} point group, but the orientation of the two pyridine rings perpendicular to each other lowers the symmetry and therefore orbital labels are excluded. Molecular orbital diagrams are given in Fig. 8 projected onto the WSW fragment orbital basis.

The HOMO and HOMO − 1 molecular orbitals for these configurations are nearly degenerate and their energies remain unchanged for both *trans*- and *cis*-configurations. Additionally, the molecular orbital diagrams show that for most occupied orbitals, energies are independent of the metal center, *i.e.*, the HOMO, HOMO − 1, HOMO − 2, and HOMO − 3 energies for $[Co(L^A)_2]^+$ show a small metal contribution and are characterized as non-bonding phenolate SALCs. The HOMO and HOMO − 1 molecular orbitals are nearly identical in energy, and it becomes clear that the observed ligand configuration is not dictated by their stabilization or destabilization. The highest occupied molecular

Table 3 Molecular orbital energies and compositions for $[Co(L^A)_2]^+$ with "*trans-phenolates*" and "*cis-phenolates*" configurations[a]

	Energy[b]		Symmetry[c]		% Metal[d]		% Ligand	
	trans	*cis*	*trans*	*cis*	*trans*	*cis*	*trans*	*cis*
LUMO + 1	−4.48	−4.39	b_{1u}	—	0.5	33.5	99.5	66.5
LUMO	−4.61	−4.51	a_g	—	67.9	32.4	32.1	67.6
HOMO	−7.86	−7.87	b_{3g}	—	8.2	5.6	91.8	94.4
HOMO − 1	−7.89	−7.88	b_{2u}	—	0.7	4.7	99.3	95.3
HOMO − 2	−8.96	−8.95	—	—	0.1	0.1	99.9	99.9
HOMO − 3	−8.97	−8.96	—	—	0.2	0.4	99.8	99.6
HOMO − 4	−9.62	−9.14	b_{2g}	—	33.6	27.7	66.4	72.3
HOMO − 5	−9.68	−9.54	b_{2u}	—	3.3	10.8	96.7	89.2

[a] The "*trans-phenolates*" configuration for $[Co(L^A)_2]^+$ is described by $[Co\langle N_{am1}N_{am2}\rangle\langle N_{py1}N_{py2}\rangle\langle O_{phen1}O_{phen2}\rangle]$, whereas the "*cis-phenolates*" configuration is $[Co\langle N_{am1}O_{phen2}\rangle\langle O_{phen1}N_{am2}\rangle\langle N_{py1}N_{py2}\rangle]$. The N_{py1}–Co–N_{py2} axis has been placed along the *z*-direction; the *y*-axis bisects the O_{phen1}–Co–O_{phen2} angle; the *x*-axis bisects the N_{am1}–Co–N_{am2} angle. [b] Energy given in eV. [c] Pseudo symmetry labels have been assigned according to the D_{2h} group. For non-bonding orbitals, pseudo symmetry labels are given only where ligand orbitals mimic symmetry adapted linear combinations. [d] "% Metal" and "% Ligand" correspond to the character of the molecular orbitals.

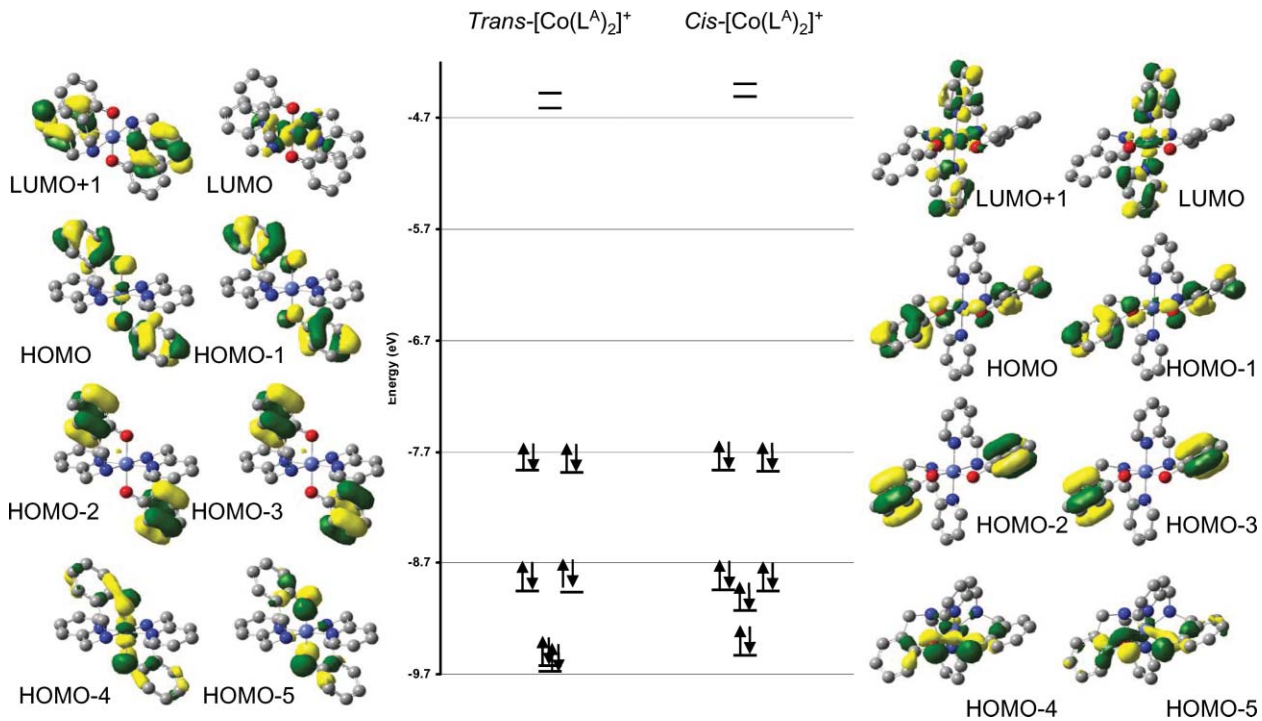

Fig. 8 (a) Molecular orbital energy level diagram for *trans*- and *cis*-$[Co(L^A)_2]^+$ and renderings of selected MOs projected onto the WSW fragment orbital basis.

orbital displaying significant metal character in both *cis*- and *trans*-phenolate structures is HOMO − 4. In the *trans*-phenolate structure this molecular orbital results from a four electron interaction between the occupied Co-centered d_{xz} orbital and occupied phenolate SALC that is commonly characterized as the in-plane O orbital. The HOMO − 4 of the *cis*-phenolate isomer is less stable by roughly 0.5 eV. This molecular orbital is derived from a two electron interaction between the unoccupied Co-centered $d_{x^2-y^2}$ orbital and the same in-plane O centered phenolate SALC. The LUMO entails 67.9% of metallic character, is labeled a_g and relates to an unoccupied $d_{x^2-y^2}$ AO, thus reinforcing the notion that in the reductive process given by Co(III) ($3d^6_{l.s.}$) + e^- → Co(II) ($3d^7$), an electron is promoted to the LUMO. It justifies the considerable changes in potential for complexes with different groups attached to the phenolate ring.

Conclusions

In order to understand and predict the properties of more complex soft materials with potential metallomesogenic properties such as compound **1**, we have investigated the behavior of five cobalt(III) complexes **2–6**. These complexes were excellent archetypes in delivering fundamental information on structural, UV-visible and redox behavior of compound **1**. Archetype **3** mimicked accurately the peak position for the $p\pi_{phenolate} \rightarrow d\sigma^*_{cobalt(III)}$ charge transfer band and metal and ligand-centered redox potentials. Based on spectroscopic and spectrometric methods, as well as by the results of our calculations and by inference from structural data for the archetypes **2**, **4**, and **6**, compound **1** should exhibit two ligands coordinated in a *trans*-configuration $[Co\langle N_{am1}N_{am2}\rangle\langle N_{py1}N_{py2}\rangle\langle O_{phen1}O_{phen2}\rangle]$, with similar bond lengths

and angles. If aiming at redox-driven switchable materials, design should be limited to systems in which *tert*-butyl and chloro groups are appended to the phenolate rings. These are the only species showing generation of phenoxyl radicals. Future work will focus on the mesogenic properties of **1** and in the development of Fe(III)-containing soft materials. Comparisons between $d^5_{high\text{-}spin}$ and $d^6_{low\text{-}spin}$ systems will be possible, as well as the understanding of the influence of *cis* and *trans* coordination of the phenolates to the metal centers. We are also investigating the cobalt archetypes of bromo- and iodo-substituted ligands that show absence of perchlorate counterions in the IR spectrum. It suggests cobalt(II) stabilization and further NMR and EPR studies are underway.

Experimental

Materials and methods

Reagents were used as received. CH_2Cl_2 was used from an Innovative Technologies solvent purification system, and MeOH was distilled over CaH_2. IR spectra were measured on a Tensor 27 FTIR-Spectrophotometer. ^{1}HNMR spectra were taken using Varian 300 and 400 mHz instruments. ESI(positive) spectra were measured in a triple quadrupole Micromass QuattroLC mass spectrometer with ESCi source. Elemental analyses were performed by Midwest Microlab, Indianapolis-IN, USA. UV-visible spectroscopy were performed on a Cary 50 spectrometer in the range 250 to 1000 nm. The samples were mortar-ground and heat-dried under vacuum overnight to eliminate solvent molecules. CV experiments were performed using a BAS 50 W voltammetric analyzer. A standard three-electrode-cell was employed with a glassy-carbon working electrode, a Pt-wire auxiliary electrode, and an Ag/AgCl reference electrode under an inert atmosphere at RT. All potentials are given *vs* Fc^+/Fc.[26] First derivative X-band EPR spectra were performed with a Bruker ESP 300 spectrometer at 120 K using liquid nitrogen as the coolant.

X-Ray structural determinations for 2, 4, and 6

All data were determined using either a Bruker P4/CCD or a Bruker X8 APEX-II kappa geometry diffractometer with Mo radiation and a graphite monochromator. Frame data were indexed and integrated with the manufacturer's software[27] and models were refined with SHELX-97.[27] Table 4 shows collection data for the three structures.

$[Co^{III}(L^{A})_2]ClO_4$ (**2**) crystallized as irregular dark fragments. A sample 0.6 × 0.4 × 0.4 mm was used for data collection at 295 K. 2450 frames were collected, yielding 8898 reflections, of which 2953 were independent. Hydrogen positions were observed and refined, including the amine proton. The cobalt atom occupies a crystallographic inversion center. The perchlorate anion is on a 2-fold axis. Diffraction data for $[Co^{III}(L^{OMeA})_2]ClO_4{\cdot}H_2O$ (**4**) were collected at 100 K on a crystal 0.15 × 0.04 × 0.02 mm. A sphere of data was measured at 20 s per frame and 0.3° between frames. 4471 frames were collected, yielding 79107 reflections, of which 7444 were independent. The hydrogen atoms were placed in observed positions and refined. The asymmetric unit contains two half-complexes, one perchlorate anion and one uncoordinated molecule of water. Both Co(III) atoms occupy inversion centers. Diffraction data for $[Co^{III}(L^{Cl2A})_2]ClO_4$ (**6**) were measured on a red irregular sample 0.18 × 0.16 × 0.15 mm at 100 K. Frames were collected as a series of sweeps with the detector at 40 mm and 0.3° between each frame. 3334 frames were collected at 10 s per frame, yielding 117026 reflections, with 14459 of them independent. Hydrogen positions were observed or calculated. The asymmetric unit consists of 2 half-complexes, one full complex and 2 perchlorate anions. Co1 and Co2 occupy inversion centers.

CCDC reference numbers 285941, 285942 and 286103.

For crystallographic data in CIF or other electronic format see DOI: 10.1039/b514190g

Syntheses

Preparation of the ligand $HL^{t\text{-}BuLC}$. A 30 mL MeOH solution of *para*-(heptyloxy) benzenaniline (0.3 g: 1.0 mmol) was treated with 2-pyridinecarboxyaldehyde (0.11 g: 1.0 mmol) at 50 °C for 2 h, yielding a pale yellow solution. $NaBH_4$ (0.56 g: 1.5 mmol) was than added at 0 °C in small portions. The solution was stirred at room temperature for 2 h, the solvent was evaporated, and the amine formed was extracted with dichloromethane, dried over $MgSO_4$ and isolated. The amine so obtained was dissolved in 30 mL

Table 4 Crystal data[a]

	$[Co^{III}(L^{A})_2]ClO_4$ (**2**)	$[Co^{III}(L^{OMeA})_2]ClO_4{\cdot}H_2O$ (**4**)	$[Co^{III}(L^{Cl2A})_2]ClO_4$ (**6**)
Formula	$C_{26}H_{26}ClCoN_4O_6$	$C_{28}H_{32}Co_1Cl_1N_4O_9$	$C_{26}H_{22}Co_1Cl_5N_4O_6$
M	584.89	662.96	722.66
Space group	*C*2/*c*	$P2_1/n$	$P2_1/n$
a/Å	20.2884(15)	11.8170(8)	11.1872(6)
b/Å	8.4867(7)	14.8833(9)	22.7813(13)
c/Å	15.4068(12)	17.2517(12)	22.1940(13)
β/°	109.344(2)	108.448(3)	98.922(2)
V/Å^3	2503.0(3)	2878.2(3)	5587.9(5)
Z	4	4	8
T/K	295(2)	100(2)	100(2)
λ/Å	0.71073	0.71073	0.71073
D_{calc}/g cm^{-3}	1.552	1.530	1.718
μ/mm^{-1}	0.843	0.751	1.143
R(*F*) (%)	3.05	3.93	3.34
Rw(*F*) (%)	7.45	8.12	7.90

[a] $R(F) = \sum\|F_o| - |F_c\|/\sum|F_o|$ for $I > 2\sigma(I)$; $Rw(F) = [\sum w(F_o^2 - F_c^2)^2/\sum w(F_o^2)^2]^{1/2}$ for $I > 2\sigma(I)$.

CH_2Cl_2, and then refluxed in the presence of 2,4-di-*tert*-butyl-6-(chloromethyl)phenol (0.26 g: 1.0 mmol) and excess of Et_3N overnight. The reaction mixture was washed with 10% $NaHCO_3$, the organic layer was isolated and dried over $MgSO_4$ and then roto-evaporated to yield the ligand $HL^{t\text{-}BuLC}$. IR data (KBr, cm^{-1}): 3456 (O–H); 2953–2859 (s) (C–H), 1608 (s), 1526 (s), 1474 (s) (C=N_{py}, C=C aromatic). ^{1}H-NMR data [400 MHz, $CDCl_3$, 300 K] δ (ppm): 0.90 [t, 3H (CH_3)]; 1.22–1.46 (overlapped m, 26H (CH_2) and s, ^{t}Bu (CH_3)]; 1.82 [m, 2H (OCH_2CH_2)]; 3.72 (s, 2H (Ph–CH_2–N–)]; 3.78 [s, 2H (N–CH_2–Ar)]; 3.9 [t, 2H (Ar–O–CH_2–)]; 4.0 [s, 2H (Py–CH_2–N–)]; 6.8 [s, 1H (aryl)]; 6.94 [d, 2H (aryl)]; 6.96 [d, 2H (aryl)]; 7.16 [d, 2H (aryl)] 7.48 [d, 2 H (aryl)]; 7.51 [d, 2 H (aryl)] 7.2–7.8 [m, 3H (pyridine)]; 8.57 [d, 1 H (pyridine)]. MS data (ESI$^+$ in MeOH): $m/z = 607$ [$HL^{t\text{-}BuLC}$ + H]$^+$.

Preparation of the ligands HL^A, $HL^{t\text{-}BuA}$, HL^{OMeA}, HL^{NO2A}, and HL^{Cl2A}. The ligands HL^A and $HL^{t\text{-}BuA}$ were obtained according to literature procedures.[29,30] The ligands HL^{OMeA}, HL^{NO2A}, and HL^{Cl2A} were synthesized according to a general procedure in which 2-aminomethyl-pyridine (1.08 g: 10.0 mmol) and the appropriate aldehyde (10.0 mmol) were condensed in 20 mL of MeOH at 40 °C. After 2 h, NaBH4 (0.5 g: 15 mmol) was added at 0 °C. The solvent was roto-evaporated and the crude product was dissolved in 100 mL of 5% aqueous $NaHCO_3$. Extraction with 4 × 25 mL of dicholoromethane took place, and the combined extracts were dried over $MgSO_4$. The solutions were concentrated and allowed to stand for several days at 0 °C giving microcrystalline solids. The characterizations follow.

HL^{OMeA} (2-methoxy-6-{[(pyridin-2-ylmethyl)-amino]-methyl}-phenol). 2-Hydroxy-3-methoxy-benzaldehyde (1.52 g: 10 mmol) was used. Yield = 2.0 g (82%); mp = oil. IR data (KBr, cm^{-1}): 3304 (O–H); 1591 (s), 1571 (m), 1464(s) (C=N_{py}, C=C aromatic); 1274 (s) (C–O). ^{1}H-NMR data [400 MHz, $CDCl_3$, 300 K] δ (ppm): 3.85, 3.92 [2 × s, 2 ×1 H (CH_2)]; 4.04 [3 × s, 3 × 1 H (CH_3)]; 6.6 [d,1 H (aryl)]; 6.7 [t,1 H (aryl)]; 7.1 [d, 1 H (aryl)]; 7.2–7.6 [m, 3 H (py)]; 8.57 [d, 1 H (py)]. EI data: m/z: 244 [HL^{OMeA}]; 152 [HL^{OMeA} – ($PyCH_2$–)]; 137 [HL^{OMeA} – ($PyCH_2NH$–)]; 107 [($PyCH_2NH$–)].

HL^{NO2A} (4-nitro-2-{[(pyridin-2-ylmethyl)-amino]-methyl}-phenol). 2-Hydroxy-5-nitro-benzaldehyde (1.67 g: 10 mmol) was used. Yield = 2.2 g (84%); mp (uncorrected) = 151–153 °C; IR data (KBr, cm^{-1}): 3305 (O–H); 1595 (s), 1570 (m), 1477(s)(C=Npy, C=C ar); 1280 (s) (C–O). ^{1}H-NMR data [400 MHz, $CDCl_3$, 300 K] δ (ppm): 3.94, 4.06 [2 × s, 2 × 1 H (CH_2)]; 6.9 [d, 1 H (aryl)]; 7.2–7.7 [m, 3 H (Py)]; 7.9 [s,1 H (aryl)]; 8.1 [d, 1 H (aryl)] 8.59 [d, 1 H (Py)]. EI data m/z: 259 [HL^{NO2A}]; 107 [($PyCH_2NH$–)].

HL^{Cl2A} (2,4-dichloro-6-{[(pyridin-2-ylmethyl)-amino]-methyl}-phenol). 3,5-Dichloro-2-hydroxy-benzaldehyde (1.91 g: 10 mmol) was used. Yield = 2.4 g (85%); mp (uncorrected) = 110–112 °C. IR data (KBr, cm^{-1}): 3427 (O–H); 1596 (m), 1573(m), 1439 (s) (C=N_{py}, C=C_{ar}); 1294 (s) (C–O). ^{1}H-NMR data [400 MHz, $CDCl_3$, 300 K] δ (ppm): 3.91, 3.97 [2 × s, 2 × 1 H (CH_2)]; 6.8 [s,1 H (aryl)]; 7.1 [s, 1 H (aryl)], 7.2–7.6 [m, 3 H (Py)]; 8.59 [d, 1 H (Py)]. MS data (ESI$^+$ in MeOH): $m/z = 283.0$ [HL^{Cl2A} + H]$^+$.

Preparation of the compound $[Co(L^{t\text{-}BuLC})_2]ClO_4$ (1). A 25 mL MeOH solution of $HL^{t\text{-}BuLC}$ (0.31 g: 0.5 mmol) and Et_3N (0.14 mL: 1.0 mmol) was treated with a 2 mL MeOH solution of $Co(ClO_4)_2{\cdot}6H_2O$ (0.10 g: 0.25 mmol). The resulting brown solution was stirred at room temperature and filtered to discard any unreacted solids after 2 h. Slow solvent evaporation yielded a brown waxy precipitate that was frit-filtered and washed with water and cold methanol and dried under vacuum. The complex was characterized by IR and UV-visible spectroscopy, and mass spectrometry. Yield 70%. IR data (KBr, cm^{-1}) 2950 (C–H stretches from alkyl chain); 1096 (Cl–O from ClO_4^-), 1608 (C=N stretch form the pyridine ring); MS data (ESI$^+$ in MeOH): $m/z = 1270$ [$Co^{III}(L^{t\text{-}BuLC})_2$]$^+$.

CAUTION! Although no difficulties were experienced, complexes **1–6** were isolated as their perchlorate salts, and therefore they should be handled as potentially explosive compounds.

Preparation of the archetypes 2–6. Due to similar procedures, a general synthetic route is described for these syntheses. A solid sample of $Co(ClO_4)_2{\cdot}6H_2O$ (0.37 g; 1.0 mmol) was added to a 30 mL MeOH solution containing 2.0 mmol of the appropriate ligand and Et_3N (0.28 mL; 2.0 mmol). After homogenization the resulting solution is stirred at room temperature for 1 h, when it is filtered to isolate any solid material. After 24 h dark brown microcrystalline precipitates were frit filtered and washed with cold water and diethyl ether, and recrystallized in MeOH by slow evaporation at ambient conditions.

*$[Co^{III}(L^A)_2]ClO_4$ (**2**).* Yield 79%. Elemental anal. calcd for $C_{26}H_{26}N_4Cl_1O_6Co_1$: C, 53.39, H, 4.48, N 9.58%. Found: C, 53.41, H, 4.53, N, 9.49%. IR data (KBr, cm^{-1}): 1092 (Cl–O from ClO_4^-), 1595 (C=N from pyridine). MS data (ESI$^+$ in MeOH): $m/z = 485$ [$Co^{III}(L^A)_2$]$^+$.

*$[Co^{III}(L^{t\text{-}BuA})_2]ClO_4{\cdot}CH_3OH$ (**3**).* Yield 78%. Elemental anal. calcd for $C_{43}H_{62}N_4Cl_1O_7Co_1$: C, 61.38, H, 7.43, N 6.66%. Found: C, 61.48, H, 7.38, N 6.77%. IR data (KBr, cm^{-1}): 1108 (Cl–O from ClO_4^-), 2867–2952 (C–H stretches from *tert*-butyl groups), 3438 (O–H stretch, broad). MS data (ESI$^+$ in MeOH): $m/z = 709$ [$Co^{III}(L^{t\text{-}BuA})_2$]$^+$.

*$[Co^{III}(L^{OMeA})_2]ClO_4{\cdot}H_2O$ (**4**).* Yield 75%. Elemental anal. calcd for $C_{28}H_{32}N_4Cl_1O_9Co_1$: C, 50.73, H, 4.87, N 8.45%. Found: C, 50.69, H, 4.90, N 8.21%. IR data (KBr, cm^{-1}) 1104 (Cl–O from ClO_4^-), 1244 (s) (C–O from methoxy groups). MS data (ESI$^+$ in MeOH): $m/z = 545$ [$Fe^{III}(L^{OMeA})_2$]$^+$.

*$[Co^{III}(L^{NO2A})_2]ClO_4$ (**5**).* Yield 73%. Elemental anal. calcd for $C_{26}H_{24}N_6Cl_1O_{10}Co_1$: C, 46.27, H, 3.58, N 12.45%. Found: C, 46.30, H, 3.54, N 12.31%. IR data (KBr, cm^{-1}) 1092 (Cl–O from ClO_4^-), 1476(s) (N=O stretch from nitro groups). MS data (ESI$^+$ in MeOH): $m/z = 575$ [$Co^{III}(L^{NO2A})_2$]$^+$.

*$[Co^{III}(L^{Cl2A})_2]ClO_4{\cdot}CH_3OH$ (**6**).* Yield 72%. Elemental anal. calcd for $C_{27}H_{26}N_4O_7Cl_5Co_1$ C, 42.97, H, 3.47, N 7.42%. Found: C, 42.91, H, 3.38, N, 7.57%. IR data (KBr, cm^{-1}) 1102 (Cl–O from ClO_4^-). MS data (ESI$^+$ in MeOH): m/z (100%) = 621 [$Co^{III}(L^{Cl2A})_2$]$^+$.

Acknowledgements

C.N.V. thanks the Wayne State University, the Donors of the ACS-Petroleum Research Fund (Grant No. 42575-G3), and the Nano@Wayne Initiative (Grant 11E420) for support. H.P.H. thanks the Institute for Scientific Computing at Wayne State University for support provided by an NSF-IGERT fellowship. The authors thank Dr L. Hryhorczuk for the measurement of the mass spectra.

References and notes

1 T. Fujigaya, D.-L. Jiang and T. Aida, *J. Am. Chem. Soc.*, 2003, **125**, 14690.
2 D. R. Talham, *Chem. Rev.*, 2004, **104**, 5479.
3 J. Park, A. N. Pasupathy, J. I. Goldsmith, C. Chang, Y. Yaish, J. R. Petta, M. Rinkoski, J. P. Sethna, H. D. Abruna, P. L. McEuen and D. C. Ralph, *Nature*, 2002, **417**, 722.
4 J. Hjelm, R. W. Handel, A. Hagfeldt, E. C. Constable, C. E. Housecroft and R. J. Forster, *Inorg. Chem.*, 2005, **44**, 1073.
5 S. Hayami, K. Danjobara, Y. Shigeyoshi, Y. Ogawa, Y. Maeda and Y. Inorg, *Chem. Commun.*, 2005, **08**, 506.
6 (*a*) S. J. Rowan and J. B. Beck, *Faraday Discuss.*, 2005, **128**, 43; (*b*) J. B. Beck and S. J. Rowan, *J. Am. Chem. Soc.*, 2003, **125**, 13922.
7 D. Mandon, A. Nopper, T. Litrol and S. Goetz, *Inorg. Chem.*, 2001, **40**, 4803.
8 T. Storr, Y. Sugai, C. A. Barta, Y. Mikata, M. J. Adam, S. Yano and C. Orvig, *Inorg. Chem.*, 2005, **44**, 2698.
9 (*a*) S. I. Kirin, P. Dübon, T. Weyhermu1ller, E. Bill and N. Metzler-Nolte, *Inorg. Chem.*, 2005, **44**, 5405; (*b*) S. I. Kirin, C. M. Happel, S. Hrubanova, T. Weyhermüller, C. Klein and N. Metzler-Nolte, *Dalton Trans.*, 2004, 1201.
10 (*a*) J. García-Tojal, B. Donnadieu, J. P. Costes, J. L. Serra, L. Lezama and T. Rojo, *Inorg. Chim. Acta*, 2002, **333**, 132; (*b*) M. Scarpellini, A. Neves, A. J. Bortoluzzi, I. Vencato, V. Drago, W. A. Ortiz and C. Zucco, *J. Chem. Soc., Dalton Trans.*, 2001, 2616; (*c*) L. Casella, M. Gullotti, A. Pintar, L. Messori, A. Rockenbauer and M. Gyor, *Inorg. Chem.*, 1987, **26**, 1031; (*d*) R. C. Burrows and J. C. Bailar, Jr., *J. Am. Chem. Soc.*, 1966, **88**, 4150.
11 See: *Chem. Rev.*, 2004, 104 for an overview of the biomimetic approach. Contributions on pages 419, 903, and 1077 are recommended.
12 Archetype **3** shows the same pattern with $m/z = 709$, 710, 711, and 712. A cluster of three peaks is seen for archetypes **2** (485, 486,487), **4** (545, 546, 547), and **5** (575, 576, 577), whereas **6** displays eight peaks (621–628) due to the isotopic contribution of the chloro groups.
13 D. L. Kepert, *Inorganic Stereochemistry*, Springer-Verlag, New York, 1982, p. 114.
14 The notation $\langle A_1B_2 \rangle$ indicates that A is *trans* to B, with A and B corresponding to the pyridine (N_{py}), amine (N_{am}), or phenolato (O_{phen}) groups. Subscripts 1 and 2 designate respectively the first and the second ligand. This concise notation saves space and was adapted by G. Miessler and D. Tarr, in *Inorganic Chemistry*, Pearson-Prentice Hall, pages 311–315, 2004 from the original work by John Bailar, Jr in *J. Chem. Educ.* 1957, **34**, 334 and 623. The link to Prof. Bailar's work has been explained by Prof. Miessler in a personal communication.
15 M. S. Shongwe, S. K. M. Al-Hatmi, H. M. Marques, R. Smith, R. Nukada and M. Mikuriya, *J. Chem. Soc., Dalton Trans.*, 2002, 4064 and references therein.
16 C. Imbert, H. P. Hratchian, M. Lanznaster, M. J. Heeg, L. Hryhorczuk, B. R. McGarvey, H. B. Schlegel and C. N. Verani, *Inorg. Chem.*, 2005, **44**, 7414.
17 A. Chakravorty and B. Behera, *Inorg. Chem.*, 1967, **06**, 1812.
18 P. Chaudhuri, C. N. Verani, E. Bill, E. Bothe, T. Weyhermueller and K. Wieghardt, *J. Am. Chem. Soc.*, 2001, **123**, 2213.
19 (*a*) A. Pui, I. Berdan, I. Morgenstern-Badarau, A. Gref and M. Perree-Fauvet, *Inorg. Chim. Acta*, 2001, **320**, 167; (*b*) H. P. Fritz and L. W. G. Vitè, *Z. Anorg. Allg. Chem.*, 1972, **392**, 271.
20 A. M. Tait, F. V. Lovecchio and D. H. Busch, *Inorg. Chem.*, 1977, **16**, 2206.
21 (*a*) F. Thomas, G. Gellon, I. Gautier-Luneau, E. Saint-Aman and J. L. Pierre, *Angew. Chem., Int. Ed.*, 2002, **41**, 3047; (*b*) Y. Shimazaki, S. Huth, A. Odani and O. Yamauchi, *Angew. Chem., Int. Ed.*, 2000, **39**, 1666; (*c*) A. Philibert, F. Thomas, C. Philouze, S. Hamman, E. Saint-Aman and J. L. Pierre, *Chem. Eur. J.*, 2003, **09**, 3803; (*d*) S. Itoh, S. Takayama, R. Arakawa, A. Furuta, M. Komatsu, A. Ishida, S. Takamuku and S. Fukuzumi, *Inorg. Chem.*, 1997, **36**, 1407; (*e*) B. A. Jazdzewski and W. B. Tolman, *Coord. Chem. Rev.*, 2000, **200–202**, 633; (*f*) J. Hockertz, S. Steenken, K. Wieghardt and P. Hildebrandt, *J. Am. Chem. Soc.*, 1993, **115**, 11222.
22 M. J. Frisch, G. W. Trucks, H. B. Schlegel, G. E. Scuseria, M. A. Robb, J. R. Cheeseman, J. A. Montgomery, T. Vreven, K. N. Kudin, J. C. Burant, J. M. Millam, S. S. Iyengar, J. Tomasi, V. Barone, B. Mennucci, M. Cossi, G. Scalmani, N. Rega, G. A. Petersson, H. Nakatsuji, M. Hada, M. Ehara, K. Toyota, R. Fukuda, J. Hasegawa, M. Ishida, T. Nakajima, Y. Honda, O. Kitao, H. Nakai, M. Klene, X. Li, J. E. Knox, H. P. Hratchian, J. B. Cross, V. Bakken, C. Adamo, J. Jaramillo, R. Gomperts, R. E. Stratmann, O. Yazyev, A. J. Austin, R. Cammi, C. Pomelli, J. W. Ochterski, P. Y. Ayala, K. Morokuma, G. A. Voth, P. Salvador, J. J. Dannenberg, V. G. Zakrzewski,S. Dapprich, A. D. Daniels, M. C. Strain, O. Farkas, D. K. Malick, A. D. Rabuck, K. Raghavachari, J. B. Foresman, J. V. Ortiz, Q. Cui, A. G. Baboul, S. Clifford, J. Cioslowski, B. B. Stefanov, G. Liu, A. Liashenko, P. Piskorz, I. Komaromi, R. L. Martin, D. J. Fox, T. Keith, M. A. Al-Laham, C. Y. Peng, A. Nanayakkara, M. Challacombe, P. M. W. Gill , B. Johnson, W. Chen, M. W. Wong, C. Gonzalez and J. A. Pople, *03, GAUSSIAN*, Gaussian Inc., C. T. Wallingford, 2003.
23 (*a*) A. D. Becke, *Phys. Rev. A*, 1988, **38**, 3098; (*b*) A. D. Becke, *J. Chem. Phys.*, 1993, **98**, 5648; (*c*) C. T. Lee, W. T. Yang and R. G. Parr, *Phys. Rev. B*, 1988, **37**, 785; (*d*) P. J. Stephens, F. J. Devlin, C. F. Chabalowski and M. J. Frisch, *J. Phys. Chem.*, 1994, **98**, 11623; (*e*) R. Ditchfield, W. R. Hehre and J. A. Pople, *J. Chem. Phys.*, 1971, **54**, 724; (*f*) M. S. Gordon, *Chem. Phys. Lett.*, 1980, **76**, 163; (*g*) P. C. Hariharan and J. A. Pople, *Theor. Chim. Acta*, 1973, **28**, 213; (*h*) P. C. Hariharan and J. A. Pople, *Mol. Phys.*, 1974, **27**, 209; (*i*) W. J. Hehre, R. Ditchfield and J. A. Pople, *J. Chem. Phys.*, 1972, **56**, 2257.
24 (*a*) H. B. Schlegel, *J. Comput. Chem.*, 1982, **3**, 214; (*b*) H. P. Hratchian and H. B. Schlegel, in *Theory and Applications of Computational Chemistry: The First 40 Years*, ed. C. E. Dykstra, K. S. Kim, G. Frenking and G. E. Scuseria, 2005, pp. 195–259.
25 M.-H. Whangbo, H. B. Schlegel and S. Wolfe, *J. Am. Chem. Soc.*, 1977, **99**, 1296.
26 R. Gagne, C. Koval and G. Licenski, *Inorg. Chem.*, 1980, **19**, 2854.
27 (*a*) *APEX-II and SMART*, Bruker AXS Inc., Madison, WI., USA, 2004; (*b*) *SHELX-97, Programs for Crystal Structure Analysis (Release 97-2),* G. M. Sheldrick, Institüt für Anorganische Chemie der Universität, D-3400 Göttingen, Germany.
28 G. Sheldrick, *SHELX-97*, University of Göttingen, Germany, 1997 and 2003.
29 (*a*) A. Horn, I. Vencato, A. J. Bortoluzzi, R. Hoerner, R. A. Silva, F. Nome, B. Spoganicz, V. Drago, H. Terenzi, M. C. B. de Oliveira, R. Werner, W. Haase and A. Neves, *Inorg. Chim. Acta*, 2005, **358**, 339; (*b*) A. Johansson, M. Abrahamsson, A. Magnuson, P. Huang, J. Maartensson, S. Styring, L. Hammarstroem, L. Sun and B. Aakermark, *Inorg. Chem.*, 2003, **42**, 7502; (*c*) S. Menage, G. Gellon, J.-L. Pierre, D. Zurita and E. Saint-Aman, *Bull. Soc. Chim. Fr.*, 1997, **134**, 785; (*d*) R. Viswanathan, M. Palaniandavar, T. Balasubramanian and P. T. Muthiah, *J. Chem. Soc., Dalton Trans.*, 1996, 2519; (*e*) R. Uma, R. Viswanathan, M. Palaniandavar and M. Lakshminarayanan, *J. Chem. Soc., Dalton Trans.*, 1994, 1219; (*f*) A. Neves, M. A. de Brito, I. Vencato, V. Drago, K. Griesar, W. Haase and Y. P. Mascarenhas, *Inorg. Chim. Acta*, 1993, **214**, 05.
30 (*a*) J. M. Mitchell and N. S. Finney, *J. Am. Chem. Soc.*, 2001, **123**, 862; (*b*) Y.-L. Wong, Y. Yan, E. S. Chan, Q. Yang, T. C. Mak and D. K. Ng, *J. Chem. Soc., Dalton Trans.*, 1998, 3057.